Polymerase ε1 mutation in a human syndrome with facial dysmorphism, immunodeficiency, livedo, and short stature ("FILS syndrome")

Jana Pachlopnik Schmid,[1,2,6] Roxane Lemoine,[1,6] Nadine Nehme,[1,6] Valéry Cormier-Daire,[3,6] Patrick Revy,[1,6] Franck Debeurme,[1,6] Marianne Debré,[2] Patrick Nitschke,[6] Christine Bole-Feysot,[6] Laurence Legeai-Mallet,[3,6] Annick Lim,[7] Jean-Pierre de Villartay,[1,2,6] Capucine Picard,[4,5,6] Anne Durandy,[1,2,5,6] Alain Fischer,[1,2,6] and Geneviève de Saint Basile[1,2,5,6]

[1]National Institute of Health and Medical Research (INSERM) Unit 768; [2]Pediatric Hematology-Immunology-Rheumatology Unit, AP-HP; [3]Department of Genetics, INSERM Unit 781; [4]Laboratory of Human Genetics of Infectious Disease, INSERM Unit 980; and [5]Study Center for Primary Immunodeficiencies, AP-HP; Necker Hospital for Sick Children, 75015 Paris, France
[6]Université Paris Descartes–Sorbonne Paris Cité, Institut *Imagine*, 75015 Paris, France
[7]Department of Immunology, Pasteur Institute, 75724 Paris, France

DNA polymerase ε (Polε) is a large, four-subunit polymerase that is conserved throughout the eukaryotes. Its primary function is to synthesize DNA at the leading strand during replication. It is also involved in a wide variety of fundamental cellular processes, including cell cycle progression and DNA repair/recombination. Here, we report that a homozygous single base pair substitution in *POLE1* (*polymerase ε 1*), encoding the catalytic subunit of Polε, caused facial dysmorphism, immunodeficiency, livedo, and short stature ("FILS syndrome") in a large, consanguineous family. The mutation resulted in alternative splicing in the conserved region of intron 34, which strongly decreased protein expression of Polε1 and also to a lesser extent the Polε2 subunit. We observed impairment in proliferation and G1- to S-phase progression in patients' T lymphocytes. Polε1 depletion also impaired G1- to S-phase progression in B lymphocytes, chondrocytes, and osteoblasts. Our results evidence the developmental impact of a Polε catalytic subunit deficiency in humans and its causal relationship with a newly recognized, inherited disorder.

CORRESPONDENCE
Geneviève de Saint Basile: genevieve.de-saint-basile@inserm.fr

Abbreviations used: EdU, 5-ethyl-2-deoxyuridine; LBL, lymphoblastoid B cell line; SNP, single nucleotide polymorphism.

DNA polymerases are required for DNA synthesis. Mutations in DNA polymerases or changes in their expression could be manifested by alterations in DNA replication, in cell cycle progression, and most prominently, in mutagenesis (Loeb and Monnat, 2008). Several different human diseases might present opportunities to identify disease-associated polymerase mutations and clarify their specific role and mechanisms. Mutations that have a strong effect on function of the canonical DNA polymerases would probably lead to early embryonal or fetal lethality. In contrast, partial loss of function or haploinsufficiency might lead to either multisystem, organ-specific, or cell lineage–specific developmental defects or to the early exhaustion of continuously replicating cell lineages.

In this study, we describe a large, consanguineous family in which mild facial dysmorphism, immunodeficiency, livedo, and short stature were associated in 11 affected subjects with genomic mutation in *POLE1* (*polymerase ε 1*), resulting in haploinsufficiency. Of note, patients did not exhibit cancer susceptibility. The findings indicate that Polε is primarily required for cell proliferation and early phase of cell cycle progression.

J. Pachlopnik Schmid and R. Lemoine contributed equally to this paper.

The Rockefeller University Press $30.00
J. Exp. Med. 2012 Vol. 209 No. 13 2323-2330
www.jem.org/cgi/doi/10.1084/jem.20121303

The Journal of Experimental Medicine

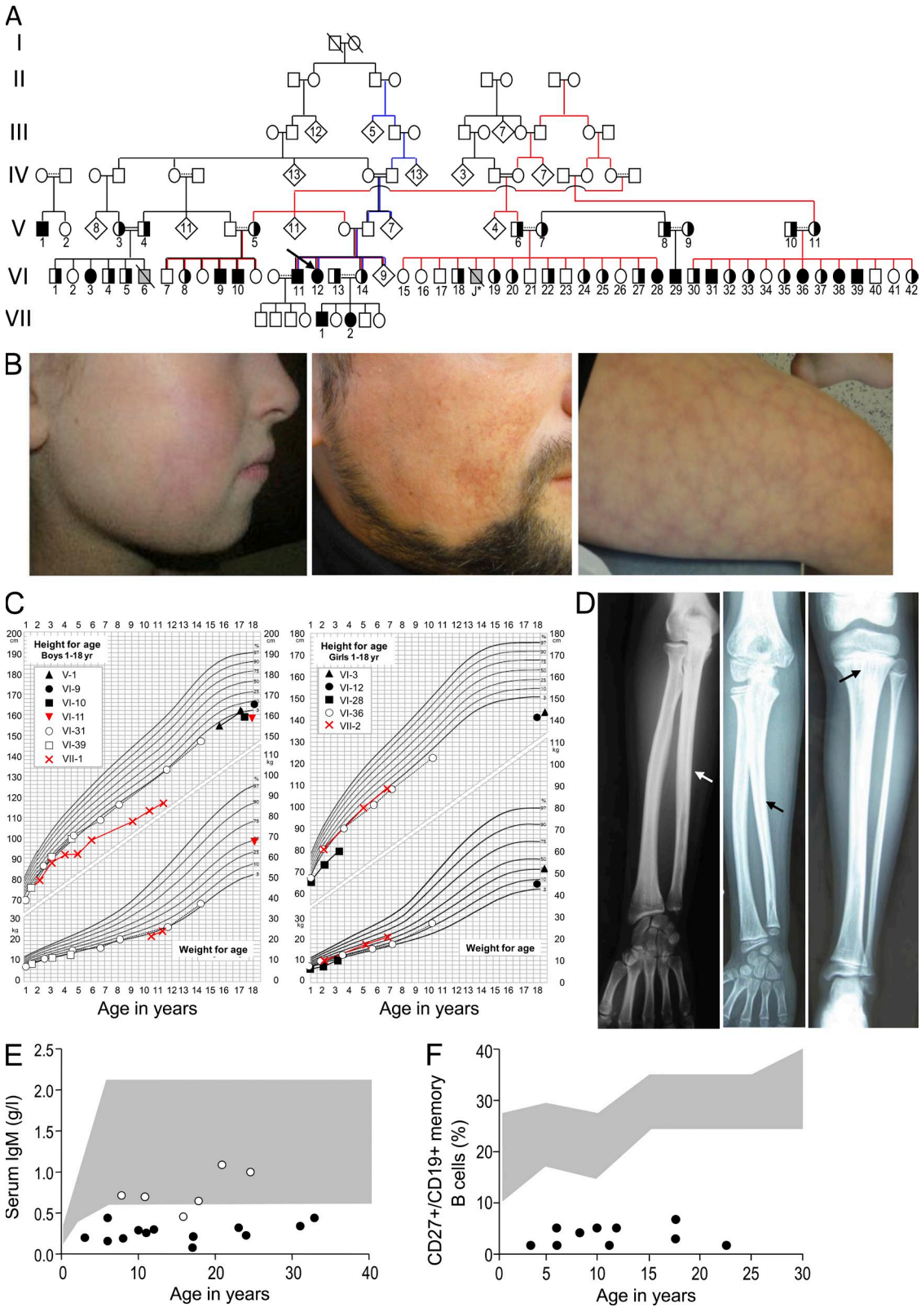

Figure 1. Pedigree and clinical manifestations in patients with the FILS phenotype. (A) Pedigree of the family with FILS. Family members having provided DNA are numbered. Completely closed symbols indicate affected individuals, and half closed symbols indicate a heterozygous carrier. An arrow designates the index case. Individuals clustered in a diamond symbol in generation IV and V were not analyzed. Gray symbols indicate patients that did not undergo genetic testing. Slashes indicate deceased persons, double horizontal lines consanguinity, and dotted lines presumed interrelations. Case J*

RESULTS AND DISCUSSION

FILS syndrome manifestations

11 members of a large, consanguineous French kindred displayed mild facial dysmorphism, immunodeficiency, livedo, and short stature (referred to by us as "FILS syndrome"). Three additional members displayed two or three of these four features. The pedigree and clinical features of the family members investigated in the present study are shown in Fig. 1, Table 1, and Table S1. One affected individual (VI-11) has four children and so the syndrome is not associated with (male) infertility (Fig. 1 A). The patients had mild facial dysmorphism with malar hypoplasia (Fig. 1 B) and a high forehead. Livedo on the cheeks, forearms, and/or legs was present in all but one patient and noticed since birth in numbers of them (Fig. 1 B). There was no ulceration. With increasing age, telangiectasia was observed on the cheeks. Patients were born at term with a normal gestational weight and length. Growth impairment was observed during early childhood and resulted in shortness of height in adulthood, though to varying degree (Fig. 1 C). The mean height of the unaffected siblings was around the 50th percentile. Growth hormone production and response were tested in three patients and found to be normal. The head circumference was normal in all but one patient (VI-3), and thus the FILS patients had a relative macrocephaly. Patients VI-3, VI-11, and VI-29 had bone dysplasia and suffered from pain in the extremities; lacunar bone lesions, cortical thickening, and modeling defects at the long bone diaphyses were found in the three patients, whereas striae in the metaphyses were observed in patient VI-3 only (Fig. 1 D).

All but two of the patients with a FILS phenotype suffered from an immunodeficiency that gave rise to medical evaluation in the index patient VI-12. Since their first year of life, patients had recurrent upper and lower respiratory tract infections, recurrent pulmonary infections resulting in two patients in bronchiectasis (patients VI-31 and VI-36), and recurrent meningitis caused by *Streptococcus pneumonia*. Patient J* died during a pulmonary infection at the age of 2 yr. Immunological experiments of the patients (Fig. 1, E and F; Table 1; and Table S1) showed decreased IgM and IgG2 levels, reduced isohemagglutinin titers, and a predominant lack of antibodies to polysaccharide antigens. Patients had low memory ($CD27^+$) B cell counts, but the proportion of switched B cells ($\mu^-\delta^-$) and nonswitched memory B cells were equally affected. The IgM, IgG, and IgA B cell repertoires in blood lymphocytes performed in one patient (VII-1) showed a normal distribution of VH family usage (not depicted). B cell proliferation and switch to IgE production were normal upon stimulation with IL-4 and CD40 ligand in vitro (not depicted). In addition, several patients had low naive T cell counts and decreased T cell proliferation (Table S1). Immunoscope analysis of T cells in one patient (VII-1) showed a normally diversified TCR Vβ repertoire (not depicted). Allergies, autoimmunity, opportunistic infections, and malignancies were not observed in these patients. Although FILS patients' phenotype resembled the one observed in Bloom's disease, sister chromatid exchange was normal.

Identification of a mutation in POLE1

To identify the causal gene underlying the FILS syndrome and based on an assumption of autosomal recessive inheritance, single nucleotide polymorphism (SNP) array genome-wide homozygosity mapping was performed. This revealed a common 2-Mb region located at the end of chromosome 12q containing 28 annotated genes, with a logarithm of the odds ratio (LOD score) of 11 (Fig. 2 A). Sequencing of the coding exons of candidate genes with functions related to cell division or cell growth, *checkpoint with forkhead associated and ring finger* (*CHFR*), *DEAD box protein 51* (*DDX51*), *Zinc finger 605* (*ZNF605*), *ZNF140*, *nucleolar complex associated 4 homologue* (*NOC4L*), and *POLE1* revealed in the 14 patients a homozygous nucleotide substitution at position 3 in intron 34 (g.G4444+3 A>G) in the *POLE1* gene (Fig. 2 A). Exome sequencing in one of the patients (VI-28) also identified this substitution and showed that *POLE1* was the only mutated gene within the defined genetic linkage region on chromosome 12q. All tested parents were heterozygous for the mutation. The mutation was absent from control populations, in-house exome sequencing data, and all publically available databases (including the dbSNP129 and 1000 Genomes datasets). Heterozygous individuals were asymptomatic.

The g.G4444+3 A>G mutation's impact on mRNA splicing was then evaluated. Using primers located in exons 32 and 37 (which thus flanked intron 34), two PCR products were separated on agarose gels from homozygous and heterozygous individuals (six patients and three parents), whereas a single band was found in control individuals (Fig. 2 B). Sequencing of the smaller PCR product (predominant in the patients) identified a *POLE1* species lacking exon 34 (Fig. 2, B and C). Sequencing of the larger PCR product identified WT *POLE1* sequence in control samples and the parents' samples and a mixed sequence in the patients' samples (Fig. 2, B and C). After amplifying and cloning the upper band from two patients (VI-39 and VII-1), we found (a) a WT sequence in 63% of 46 clones and (b) deletion of exon 34 in 30% of them. Two other clones had different frame-shifted insertions and deletions.

died after a pulmonary infection at the age of 2 yr. (B) Facial profile photographs showing patient VI-36 at the age of 9, with livedo on the cheek and discrete malar hypoplasia (left), telangiectasia on the cheek of patient VI-11 at the age of 33 (middle) and, lastly, livedo on the thigh of patient VI-11 (right). (C) Growth charts for male (left) and female (right) patients, showing short stature in all instances and particularly substantial growth impairment in patients VI-3, VI-10, VI-11, VI-12, VI-28, and VII-1. (D) X ray of the forearm of case VI-3 (left) and patient VI-29 (middle) showing irregular diaphyseal hyperostosis (arrows) and x-ray of the leg of patient VI-29 (right) showing irregular diaphyseal hyperostosis and metaphyseal striations (arrow). (E) IgM levels in patients (closed dots) and heterozygous individuals (open dots) of different ages. The shaded area indicates our in-house normative values. (F) Percentages of memory B cells ($CD27^+/CD19^+$) in patients (closed dots). The shaded area indicates normal level from in-house control values.

Table 1. Clinical and laboratory summary of the FILS patients

Parameter	Patient ID													
	V-1	VI-3	VI-9	VI-10	VI-11	VI-12	VI-28	VI-29	VI-31	VI-36	VI-38	VI-39	VII-1	VII-2
Gender	m	f	m	m	m	f	f	m	m	f	f	m	m	f
Age at last follow up (yr)	17	23	25	24	33	31	3	11	17	10	8	6	11	6
Recurrent respiratory infections	+	+	+	+	−	+	+	+	+	+	−	+	+	+
Facial dysmorphy	+	+	+	+	+	+	+	−	+	+	+	+	+	+
Livedo	+	+	+	+	+	+	+	−	+	+	+	+	+	+
Bone disease	−	+	−	−	+	−	−	+	−	−	−	−	−	−
Short stature	(+)	+	−	+	+	++	++	(+)	(+)	+	nd	(+)	++	(+)
IgM	↓	↓	nd	↓	↓	↓	↓	↓	↓	↓	↓	↓	↓	↓
Anti–*S. pneumoniae* polysaccharide IgG	↓	nd	nd	nd	nd	nd	↓	nd	↓	↓	↓	↓	↓	↓

f, female; m, male; nd, not done. For Short stature, "+" indicates less than −2 SD; "(+)" indicates −2 SD; and "++" indicates −4 SD or less. For IgM, "↓" indicates below −2 SD. For Anti–*S. pneumoniae* polysaccharide IgG, "↓" indicates antibody titer increase after nonconjugate anti-pneumococcal 23-valent vaccine less than fourfold.

Thus, individuals with the g.G4444+3 A>G substitution have two major *POLE1* transcripts: WT and exon 34 deleted (Fig. 2 C). The proportion of the WT *POLE1* transcript in T lymphoblasts was significantly lower in patients (by around 90%) than in control individuals, whereas the total overall amount of *POLE1* transcripts did not differ significantly as determined by quantitative PCR. These data confirm that the major transcript in FILS patients was exon 34 del *POLE1*.

Impaired expression of POLε1 and POLε2

The 49 coding exons of *POLE1* are translated into a 2,286-residue protein. It comprises a large N-terminal catalytic domain with exonuclease and polymerase motifs and a C-terminal domain containing binding sites for the small subunits of the Polε holoenzyme. Deletion of *POLE1* exon 34 would lead to a subsequent frame shift (from S1483V onwards) and a premature stop codon at position 1561 in the new protein, which would thus lack the C-terminal half (Fig. 2 D). However, we could not detect any truncated protein in lymphocyte samples (from five patients and three heterozygous individuals). In contrast, severely decreased expression of full-length Polε1 was found in the patients and, to a lesser extent, in the heterozygous individuals (Fig. 2 E). In addition to Polε1, the Polε holoenzyme comprises three additional subunits: Polε2, Polε3, and Polε4. It has been assumed that Polε2 stabilizes the catalytic Polε1 (Li et al., 1997). Polε2, Polε3, and Polε4 also interact with other proteins and with DNA (Dua et al., 1999; Li et al., 2000; Shikata et al., 2006; Bermudez et al., 2011) and are thus likely to influence the holoenzyme's functional state. We therefore investigated the expression of the other three Polε subunits. There were no significant differences between patients and controls in terms of the transcript levels of *POLE2*, *POLE3*, and *POLE4* (not depicted). In contrast, protein expression of Polε2 was found to be abnormally low, supporting a role in turn of the catalytic subunit in stabilizing Polε2 (not depicted; Li et al., 1997). Protein expression of Polε3 was normal (not depicted). Protein expression of Polε2 was also subnormal in heterozygous individuals but was not as low as in the patients (not depicted).

Impaired proliferation and cell cycle progression of Polε–deficient cells

In eukaryotes, DNA polymerases α, δ, and ε jointly enable DNA replication (Hubscher et al., 2002). DNA replication is initiated by the Polα–primase complex, which synthesizes short, primed templates. Next, Polε and Polδ tether to primed templates and are thought to replicate the leading and lagging strands, respectively (Loeb and Monnat, 2008). To assess the *POLE1* mutation's cellular consequences, we used a sequential CFSE dilution assay to analyze the T lymphocytes' ability to proliferate in response to anti-CD3 and IL-2 stimulation. In contrast, to control lymphocytes, a significant proportion of the patients' T lymphocytes had not divided at day 4 (Fig. 3 A). This was not a consequence of defective cell activation or elevated cell death because the proportion of CD25- and annexin-V–positive cells, respectively, were similar in cell samples from patients and controls (not depicted). We next looked at whether low Polε1 levels modified the cell cycle progression. A cell cycle distribution analysis was performed using propidium iodide and 5-ethyl-2-deoxyuridine (EdU) labeling in primary T lymphoblasts from seven patients and in a lymphoblastoid B cell line (LBL) from patient VI-29. We observed a strikingly higher proportion of Gap 1 (G1)–phase nuclei in CD4 and CD8 T lymphocytes from the patients and a corresponding lower proportion of synthesis (S)-phase nuclei, when compared with WT controls (Fig. 3 B). Similar results were obtained with the patient VI-29 LBL, whereas LBL from a heterozygous subject (V-9) displayed an intermediate phenotype (Fig. 3 C). This phenotype was dramatically exacerbated when the residual level of Polε1 protein expressed in VI-29 LBL cells was reduced

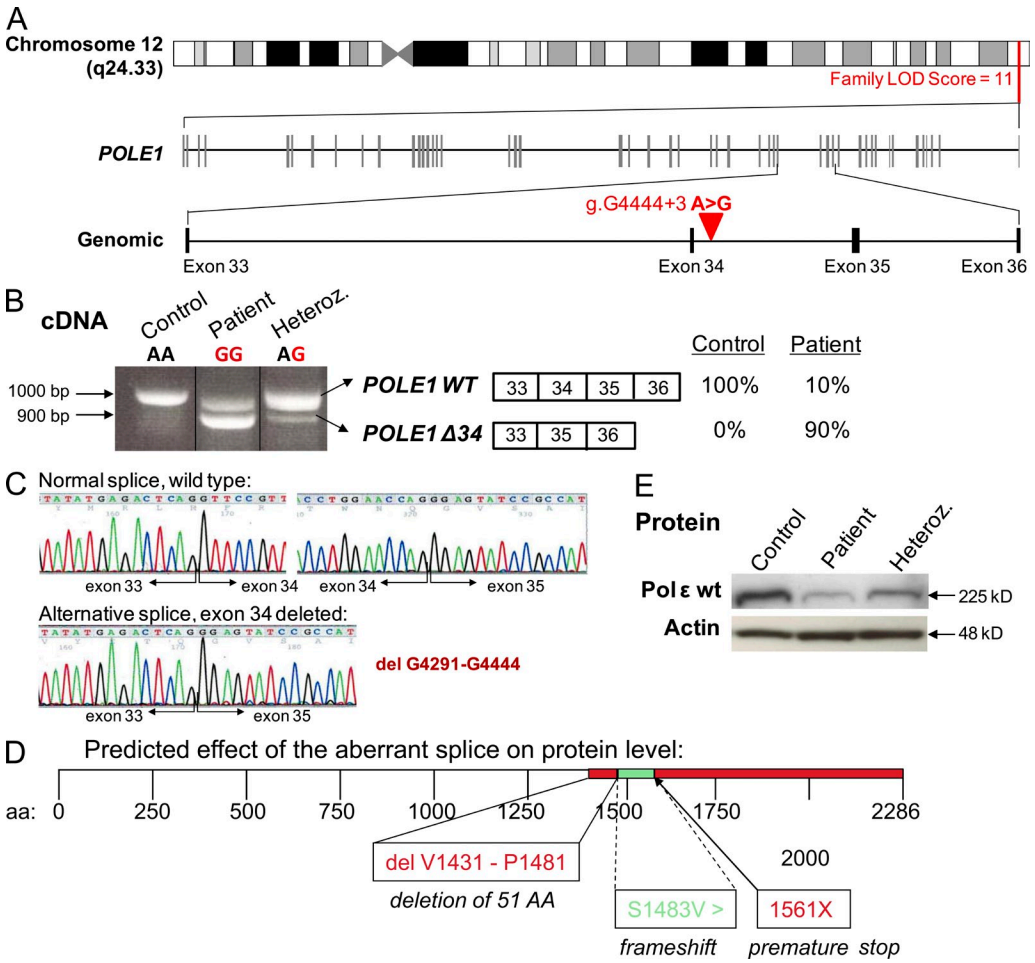

Figure 2. Homozygous single base pair substitution in *POLE1*. (A) Schematic representation of the candidate interval on the long arm of chromosome 12 defined by linkage analysis and the intronic nucleotide substitution (g.G4444+3 A>G) between exons 34 and 35. (B) At the cDNA level, the mutation results in two distinct *POLE1* transcripts, a WT transcript (*POLE1* WT) and a transcript deleted of exon 34 (*POLE1* Δ34), accounting for 10% and 90% of the *POLE1* transcript expressed in patients cells, respectively. (C) Electropherograms of *POLE1* cDNA obtained by sequencing the upper and lower bands, highlighting the exon 34 deletion in the lower band (bottom left). (D) Schematic representation of the predicted effect of the aberrant splice on the Pole1 protein. The intronic mutation results in an alternative splice, which deletes 51 aa in the WT protein leading to frameshift and premature stop codon at position 1561. (E) Polε1 protein levels in LBLs from a FILS patient (VI-29) and a heterozygous individual (V-9) compared with a control subject. Actin was used as a loading control. This Western blot is representative of three experiments.

further by *POLE1* shRNA (Fig. 3, D and E). Thus, the observed phenotype correlated with the extent of *POLE1* transcript depletion. Given the short stature displayed by the patients affected by FILS syndrome and the bone anomalies observed in some of the individuals, we also looked at whether *POLE1* depletion also affected cell cycle progression in chondrocyte and osteoblast cell lines. Indeed, a similar impairment in the G1- to S-phase transition was observed in both cell lines after Polε1 depletion with a specific shRNA (Fig. 3 F and not depicted). To determine whether *POLE1* was sufficient to explain the patients' functional defects, we reconstituted *POLE1* expression by lentiviral transduction of patient LBLs. WT *POLE1* expression in the patient LBLs restored S-phase progression to a level similar to the one observed in control LBLs (Fig. 3 G). Expression of an empty vector had no effect (not depicted).

Polε and Polδ expression in various cell types

The fact that yeast Polε mutants are viable (Kesti et al., 1999) suggests that another polymerase can perform support replication of leading strand in some contexts. Polδ is a likely candidate. We investigated the distribution of *POLE1* and *POLD* transcript expression in various human cell types and found that the relative expression of *POLE1* to *POLD* was higher in PBMCs, chondrocytes, osteoblasts, osteoclasts, B cells, and testis cells than in the other cell types analyzed (Fig. 3 H). This differential expression may contribute to the tissue-specific consequences of the low Polε1 levels found in affected individuals. Of note, *POLE1* is much higher expressed in B lymphocytes than in T lymphocytes, which may account for the more sever B cell than T cell defect that characterized the patients' phenotype. Polδ expression by VI-29 LBL was comparable with control (not depicted).

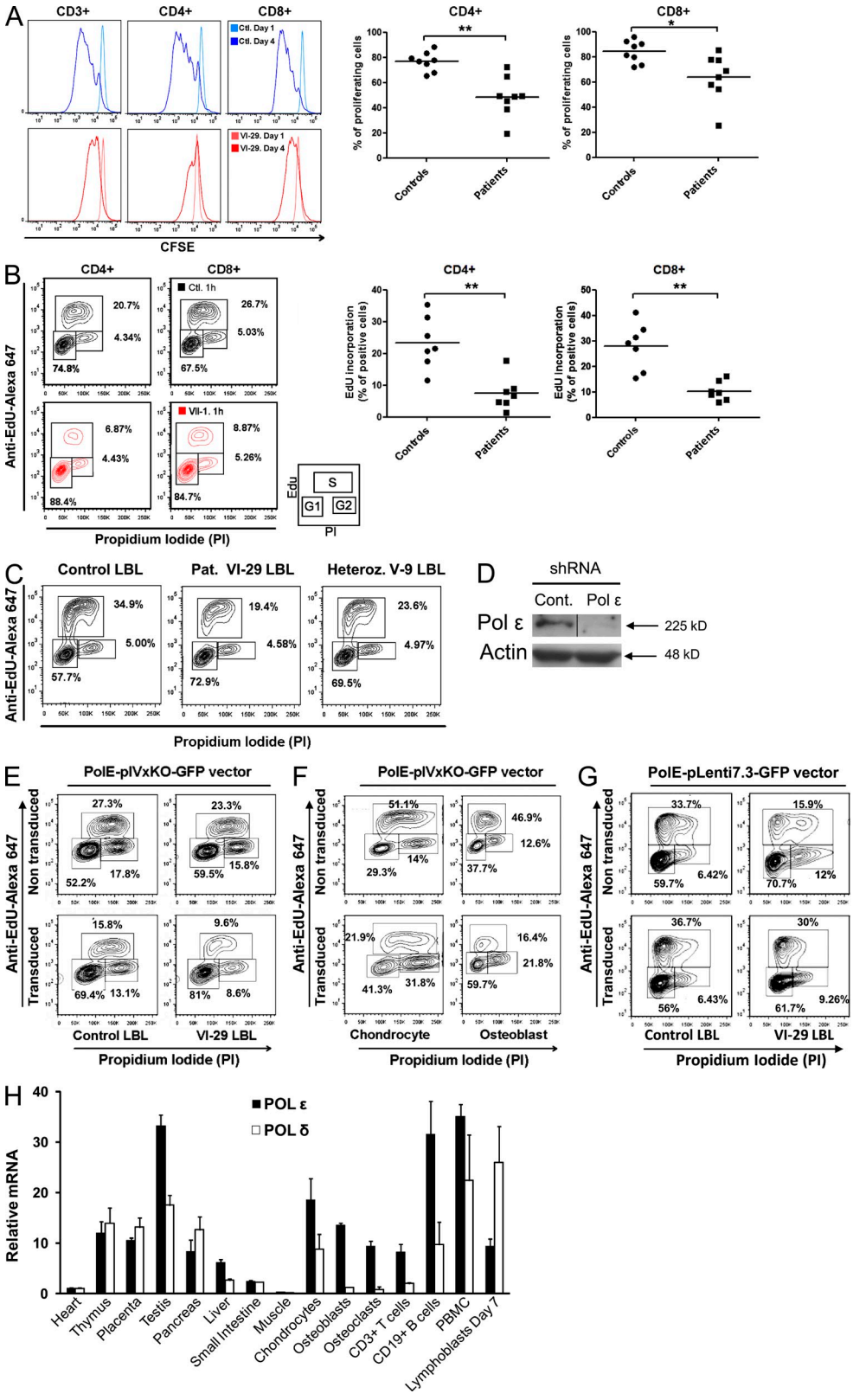

Figure 3. Impaired proliferation and cell cycle kinetics in Polε1-deficient cells. (A) Proportions of proliferating CD4+ and CD8+ T cells at day 4 after CFSE labeling and OKT3/IL-2 stimulation. Each point represents one patient (*, $P < 0.05$; **, $P < 0.005$). (B) Quantification of EdU incorporation by CD4+ and CD8+ T cells obtained from controls and FILS patients. Each point represents one patient (**, $P < 0.005$). The cell cycle was measured by EdU incorporation and propidium iodide labeling of cells cultured for 5 d after stimulation with aCD3/CD28 beads. Cells were labeled with EdU for 1 h before

This study is the first to report an association between a mutation in the *POLE1* gene and a human disorder. Mice with disruption of *Pole1* gene die in utero (Mouse Genome Informatics, http://www.informatics.jax.org/marker/MGI:1196391), whereas those with knockin allele resulting in loss of Polε proofreading, while retaining polymerase activity, die prematurely of intestinal adenomas and adenocarcinomas (Albertson et al., 2009). The splice mutation observed here was associated with residual expression of ∼10% of normal protein levels. Affected family members do not exhibit cancer susceptibility. Nonetheless, FILS patients had congenital abnormalities, including mild facial dysmorphic features, immunodeficiency, livedo, and short stature. Decreased expression of Polε1 primarily results in alteration of the cell cycle kinetics, with a prolonged G1 phase, delayed S-phase entry, and thus restricted cell proliferation. This phenotype was observed in all cell types tested, including the T and B lymphocytes, chondrocytes, and osteoblasts that strongly express Polε1 and are relevant to the manifestations in FILS syndrome. We found that Polε1 promotes S-phase entry in these cells, rather than S-phase progression as previously reported in fibroblasts (Bermudez et al., 2011). Although residual Polε1 protein expression and the potential redundancy with Polδ function may explain the partially preserved cell growth, a partial Polε1 deficiency appears to have important developmental consequences. Further studies are needed to provide details of the mechanisms by which lymphocytes, mostly B lymphocytes, cartilage, and bone cells (chondrocytes and osteoblasts) and possibly endothelial cells are affected by low Polε1 protein levels. These findings suggest that patients with a FILS phenotype could be usefully screened for mutations in the genes encoding Polε1 and the other subunits of the Polε complex.

MATERIALS AND METHODS

SNP linkage analysis and sequence analysis. Genomic DNA was isolated by phenol/chloroform extraction. A genome-wide linkage study was performed using Affymetrix GeneChip Mapping 250 K NspI as described elsewhere (Côte et al., 2009). Homozygous regions were detected using a parametric, SNP-based linkage analysis (MERLIN software, version 1.1.1). Genomic DNA and cDNA were amplified, sequenced, and analyzed on an ABI Prism 3700 system (using a BigDye Terminator sequencing kit; Applied Biosystems). The impact of the intronic mutation on splicing was analyzed using primers located on exons 32 and 37 to amplify cDNA (Table S2). Exome sequencing analysis of a DNA sample from a FILS patient was performed as described elsewhere (Le Goff et al., 2012).

Growth charts. Curves were adapted from the World Health Organization growth charts (Braegger et al., 2011).

Cell cultures. Lymphoblasts were obtained by incubating PBMCs for 72 h with PHA (1:400 dilution; Sigma-Aldrich) and 20 IU/ml IL-2 (PeproTech) in Panserin medium (Biotech GmbH) supplemented with 10% human AB serum (Etablissement Français du Sang). Proliferation and IgE class switch recombination in blood lymphocytes were assessed after activation with 500 ng/ml sCD40 Ligand (Amgen) and 100 U/ml IL-4 (R&D Systems) as described elsewhere (Imai et al., 2003). Primary human chondrocytes and osteoblasts were immortalized by transfection with Simian virus 40 large T-antigen (SV40-TAg) as previously reported (Benoist-Lasselin et al., 2007). Osteoclasts were obtained from human PBMCs in the presence of M-CSF and RANKL (Chabbi-Achengli et al., 2012). Osteoclast mRNA was provided by M.C. de Vernejoul (INSERM U606 and Université Paris Descartes–Sorbonne Paris Cité, Paris, France).

Detection of apoptotic cells with annexin-V. The proportion of viable cells was determined by using the Annexin-V PE Apoptosis Detection kit I (BD). Cell fluorescence was measured on a FACSCanto (BD).

Gene expression analysis. Total RNA was isolated from the different cell types using the RNeasy Mini kit (QIAGEN), depleted in genomic DNA, and then reverse-transcribed into cDNA using QuantiTect (QIAGEN). Quantitative PCR was performed on cDNA using SYBR Green PCR Master mix (Applied Biosystems) and *POLE1*- and actin-specific primers (Table S2). Fluorescence during PCR and subsequent dissociation was measured in triplicates on an ABI 7900 cycler and analyzed using Sequence Detection Systems software (version 2.2.2; Applied Biosystems).

Protein blotting. Lymphoblasts were lysed in radioimmunoprecipitation (RIPA)/glycerol buffer (50 mM Hepes, 150 mM NaCl, 10% glycerol, 1% Triton X-100, 2 mM EDTA, and 1% sodium deoxycholate) supplemented with protease (Roche) and phosphatase (Sigma-Aldrich) inhibitors. Cell extracts were separated by SDS-PAGE, blotted, and then stained with anti-Polε antibody 3C5.1 (Santa Cruz Biotechnology, Inc.), anti-Polε2 antibody clone 1A3 (Abcam), and anti-Polε3 antibody (Bethyl Laboratories, Inc). Anti-Polε4 antibody (Abnova) did not detect any proteins at the expected position (12 kD) in lymphocyte cell lysates from healthy individuals. Thus, the results are not shown. After staining with an HRP-conjugated secondary antibody, the immunoblot was developed with an Enhanced Chemiluminescence Detection kit (GE Healthcare). The intensity of the immunoblot bands was quantified using Photoshop software (Adobe).

Flow cytometry. Antibodies were purchased from eBioscience or BD; standard flow cytometry methods were used for staining cell surface markers. For B cell analysis, blood lymphocytes were stained with allophycocyanin anti-CD19 (BD), FITC–anti-CD27 (BD), biotin anti-IgM (Jackson ImmunoResearch Laboratories, Inc.), streptavidin-PerCP antibody (BD), and R-PE–anti-IgD (Harlan Sera-Lab). Data were collected on a FACSCanto system and analyzed with FlowJo 8.8.4 software (Tree Star).

fluorescence-activated cell sorting analysis. Cells in the G1 phase enter early S phase (2N) and progress to late S phase (4N) and G2 phase. Gates defined the percentage of cells in G1, S (EdU positive), and G2 phases, as presented in the inset. (A and B) Horizontal lines indicate the mean. (C) Cell cycle distribution of LBLs from patient VI-29, his parent (V-9), and a control. Data are representative of five independent experiments. (D) Polε1 protein levels in LBLs transfected with specific shRNA targeting POLε1 or control shRNA. Actin was used as loading control. The black line indicates that intervening lanes have been spliced out. (E) Effect of depleting POLε1 by specific shRNA (PolE-plVxKO-GFP vector) on the accumulation of cells in G1 phase in LBLs from a FILS patient and a control. The cell cycle in LBLs was measured by EdU incorporation after 72 h of transduction with specific shRNA (PolE-plVxKO-GFP vector). (F) Effect of depleting POLε1 by specific shRNA (PolE-plVxKO-GFP vector) on the cell cycle progression (as measured by EdU incorporation) in SV40-TAg–chondrocytes and SV40-TAg–osteoblasts. (G) Complementation of cell cycle progression by lentiviral transduction of LBLs from a FILS patient (VI-29) with WT *POLE1* (PolE-pLenti7.3-GFP vector) as compared with nontransduced cells in the same experiment. Data are representative of three independent experiments. (H) Relative amounts of *POLE* and *POLD* transcript levels in different tissues, as measured by quantitative RT-PCR and normalized against the housekeeping gene *GAPDH*. Values represent mean ± SD calculated from two independent experiments.

Proliferation assays. Proliferative responses of patients' PBMCs were determined on PBMCs purified by density gradient centrifugation and cultured for 3 d with 5 µg/ml PHA and for 5 d with 0.125 lf/ml tetanus toxoid antigen (Statens Serum Institut). [^{3}H]thymidine was added for the last 18 h. Cell proliferation was determined as cpm of [^{3}H]thymidine incorporation. Proliferation was monitored by labeling T cells with 10 µM CFSE (Invitrogen) before stimulation with anti-CD3 (OKT3: 50 ng/ml) and 50 U/ml IL2, in accordance with the manufacturer's instructions.

Cell cycle analysis. Cell cycle analyses were performed by measuring incorporation of the nucleoside analogue EdU into newly synthesized DNA 5 d after stimulation by anti-CD3/CD28 beads, in accordance with the manufacturer's instructions (Click-iTEdU; Invitrogen). EdU incorporation was measured according to the abundance of a fluorescent product and analyzed on a FACSCanto system with FlowJo 8.8.4 software.

RNA interference and complementation. For RNAi gene silencing of *POLE1*, the backbone of the replication-incompetent pLKO.1 lentiviral vector (Addgene) containing *POLE1* shRNA or scramble shRNA sequence (Thermo Fisher Scientific) was used (specific primers in Table S2). For rescue experiments, full-length *POLE1* cDNA clone was purchased from Thermo Fisher Scientific (clone ID 100069130) and subcloned into the SpeI and PstI restriction sites of the pLenti7.3/V5-TOPO plasmid (Invitrogen). Empty vector was used as control. Lentiviral particles were obtained after transient transfection of each construct into HEK293T cells (70% confluent) with Lipofectamine 2000 (Invitrogen) according to the manufacturer's instructions. LBLs, SV40-Tag–chondrocytes, and SV40-Tag–osteoblasts were transduced with *POLE1* or scramble shRNA and LBLs with WT *POLE1* lentiviral supernatants or the empty vector, and cell cycle analysis was performed 72 h after transduction.

Statistical analysis. Analyses were performed with Prism version 4 for Macintosh (GraphPad Software). Statistical hypotheses were analyzed using Student's *t* tests.

Accession codes. The references sequences in this study are available from GenBank or the NCBI Protein database under the following accession codes: *POLE* cDNA, NM_006231.2; POLE protein, NP_006222.2; *POLE2* cDNA, NM_001197330; *POLE3* cDNA, NM_017443; and *POLE4* cDNA, NM_019896.2.

Study approval. Clinical information and blood samples were collected from the patients, their relatives, and control individuals after the provision of informed consent and in respect to the Helsinki declaration. All protocols were approved by the Institut National de la Santé et de la Recherche Médicale's institutional review board.

Online supplemental material. Table S1 shows immunological features of FILS cases. Table S2 lists *POLE1* primers. Online supplemental material is available at http://www.jem.org/cgi/content/full/jem.20121303/DC1.

We are grateful to the patients with FILS syndrome and their families for participation in this study. We thank Marie Christine de Vernejoul for providing us osteoclast mRNA and Nathalie Lambert, Monique Forveille, Sonia Luce, Corinne Jacques, Chantal Harre, Aminata Diabate, Sevgen Tanir, Stéphanie Ndaga, Solenn Pruvost, and Mohammed Zarhate for their technical assistance.

This research was supported by Institut National de la Santé et de la Recherche Médicale and advanced grant of the European Research Council (PIDImmun [n°249816]) and the *Imagine* Foundation. J. Pachlopnik Schmid is funded by the Swiss National Science Foundation, and N. Nehme has received a postdoctoral fellowship from the Association pour la recherche sur le cancer.

The authors have no competing financial interests to declare.

Submitted: 15 June 2012
Accepted: 6 November 2012

REFERENCES

Albertson, T.M., M. Ogawa, J.M. Bugni, L.E. Hays, Y. Chen, Y. Wang, P.M. Treuting, J.A. Heddle, R.E. Goldsby, and B.D. Preston. 2009. DNA polymerase epsilon and delta proofreading suppress discrete mutator and cancer phenotypes in mice. *Proc. Natl. Acad. Sci. USA*. 106:17101–17104. http://dx.doi.org/10.1073/pnas.0907147106

Benoist-Lasselin, C., L. Gibbs, S. Heuertz, T. Odent, A. Munnich, and L. Legeai-Mallet. 2007. Human immortalized chondrocytes carrying heterozygous FGFR3 mutations: an in vitro model to study chondrodysplasias. *FEBS Lett.* 581:2593–2598. http://dx.doi.org/10.1016/j.febslet.2007.04.079

Bermudez, V.P., A. Farina, V. Raghavan, I. Tappin, and J. Hurwitz. 2011. Studies on human DNA polymerase epsilon and GINS complex and their role in DNA replication. *J. Biol. Chem.* 286:28963–28977. http://dx.doi.org/10.1074/jbc.M111.256289

Braegger, C., O. Jenni, D. Konrad, and L. Molinari. 2011. Neue Wachstumskurven für die Schweiz. *Paediatrica*. 1:9–11.

Chabbi-Achengli, Y., A.E. Coudert, J. Callebert, V. Geoffroy, F. Côté, C. Collet, and M.C. de Vernejoul. 2012. Decreased osteoclastogenesis in serotonin-deficient mice. *Proc. Natl. Acad. Sci. USA*. 109:2567–2572. http://dx.doi.org/10.1073/pnas.1117792109

Côte, M., M.M. Ménager, A. Burgess, N. Mahlaoui, C. Picard, C. Schaffner, F. Al-Manjomi, M. Al-Harbi, A. Alangari, F. Le Deist, et al. 2009. Munc18-2 deficiency causes familial hemophagocytic lymphohistiocytosis type 5 and impairs cytotoxic granule exocytosis in patient NK cells. *J. Clin. Invest.* 119:3765–3773. http://dx.doi.org/10.1172/JCI40732

Dua, R., D.L. Levy, and J.L. Campbell. 1999. Analysis of the essential functions of the C-terminal protein/protein interaction domain of *Saccharomyces cerevisiae* pol epsilon and its unexpected ability to support growth in the absence of the DNA polymerase domain. *J. Biol. Chem.* 274:22283–22288. http://dx.doi.org/10.1074/jbc.274.32.22283

Hubscher, U., G. Maga, and S. Spadari. 2002. Eukaryotic DNA polymerases. *Annu. Rev. Biochem.* 71:133–163. http://dx.doi.org/10.1146/annurev.biochem.71.090501.150041

Imai, K., G. Slupphaug, W.I. Lee, P. Revy, S. Nonoyama, N. Catalan, L. Yel, M. Forveille, B. Kavli, H.E. Krokan, et al. 2003. Human uracil-DNA glycosylase deficiency associated with profoundly impaired immunoglobulin class-switch recombination. *Nat. Immunol.* 4:1023–1028. http://dx.doi.org/10.1038/ni974

Kesti, T., K. Flick, S. Keränen, J.E. Syväoja, and C. Wittenberg. 1999. DNA polymerase epsilon catalytic domains are dispensable for DNA replication, DNA repair, and cell viability. *Mol. Cell.* 3:679–685. http://dx.doi.org/10.1016/S1097-2765(00)80361-5

Le Goff, C., C. Mahaut, A. Abhyankar, W. Le Goff, V. Serre, A. Afenjar, A. Destrée, M. di Rocco, D. Héron, S. Jacquemont, et al. 2012. Mutations at a single codon in Mad homology 2 domain of SMAD4 cause Myhre syndrome. *Nat. Genet.* 44:85–88. http://dx.doi.org/10.1038/ng.1016

Li, Y., H. Asahara, V.S. Patel, S. Zhou, and S. Linn. 1997. Purification, cDNA cloning, and gene mapping of the small subunit of human DNA polymerase epsilon. *J. Biol. Chem.* 272:32337–32344. http://dx.doi.org/10.1074/jbc.272.51.32337

Li, Y., Z.F. Pursell, and S. Linn. 2000. Identification and cloning of two histone fold motif-containing subunits of HeLa DNA polymerase epsilon. *J. Biol. Chem.* 275:31554.

Loeb, L.A., and R.J. Monnat Jr. 2008. DNA polymerases and human disease. *Nat. Rev. Genet.* 9:594–604. http://dx.doi.org/10.1038/nrg2345

Shikata, K., T. Sasa-Masuda, Y. Okuno, S. Waga, and A. Sugino. 2006. The DNA polymerase activity of Pol epsilon holoenzyme is required for rapid and efficient chromosomal DNA replication in *Xenopus* egg extracts. *BMC Biochem.* 7:21. http://dx.doi.org/10.1186/1471-2091-7-21